Kinetic Approach for the Study of Noncovalent Interaction between [Ru(NH$_3$)$_5$pz]$^{2+}$ and Gold Nanoparticles

E. Grueso,[†] D. Alcantara,[‡] J. Martinez,[‡] M. Mancera,[§] S. Penades,[⊥] F. Sanchez,[†] and R. Pradogotor*,[†]

Department of Physical Chemistry, Faculty of Chemistry, University of Sevilla, C/Profesor García González s/N 41012 Sevilla, Spain, Grupo Carbohidratos, Laboratory of Glyconanotechnology IIQ, CSIC-University of Sevilla, Américo Vespucio nr. 49, 41092 Sevilla, Spain, Departamento de Química Orgánica y Farmacéutica, University of Sevilla, C/Profesor García González s/N 41012 Sevilla, Spain, and CIC−BiomacGUNE, Parque tecnológico de San Sebastián, Paseo Miramón 182, San Sebastián 29009, Spain

Gold nanoparticles (AuNPs) capped with *N*-(2-mercaptopropionyl)glycine have been used to study the strength and character of the binding of a cationic metal complex, [Ru(NH$_3$)$_5$pz]$^{2+}$ (pz = pyrazine), at pH = 8, to these nanoparticles. The strength of the binding has been studied using a kinetic approach consisting of the study of the kinetics of the oxidation of this ruthenium complex by S$_2$O$_8^{2-}$ at different NaCl concentrations. When the ionic strength increases, the strength of the binding decreases, as a consequence of the partial neutralization of the charge on the AuNPs which, at pH = 8, has the tiopronin residue negatively charged. The increase of the ionic strength also produces a change in the character of the binding, which changes from anticooperative to noncooperative when the ionic strength increases. The nonelectrostatic and electrostatic components of the free energy of binding are determined. From the latter, we have obtained the values of the electrostatic potential differences at the AuNPs/solutions interface.

Introduction

A great number of applications in the nanotechnology research area are directly related to metal nanoparticles linked with sugars,[1] proteins,[2] dendrimers,[3] surfactants,[4] small ligands,[5] or DNA.[6] These nanoparticles are being used for assembling new materials, developing bioassays, and as multivalent systems for interaction studies. These interactions correspond in most cases to noncovalent interactions, that is, interactions between chemical species other than covalent bonds.

Nanoparticles are characterized by the properties of the metal cluster core but also by the organic molecules that constitute the monolayer. The variety of these nanometer-sized metallic particles depends not only on the metal nature but also on the capping agents. Among them, alkanethiolate nanoparticles have received considerable attention due to their advantages of stability, suspendability in different solvents, and facile characterization by standard analytical techniques.[7] In this sense, gold nanoparticles (AuNPs) capped with tiopronin are really stable and present a surface charge density which is function of the pH of the medium. That is, the tiopronin ligand permits one to control the surface charge on the gold nanoparticle and therefore to modulate the interaction between the AuNPs and ligands.

Although direct applications of these Au@tiopronin nanoparticles have been recently described, for example, as cell targeting,[8] there are no systematic studies in relation to the strength and character of the binding of AuNPs to small charged

ligands through noncovalent interactions. Generally speaking, these noncovalent interactions between two species produce a change in their properties. So, the union of a substrate, S, to a receptor, R, promotes a change in the free energy of the substrate given by[9]

$$\Delta G_S = RT \ln \gamma_S \tag{1a}$$

$$\gamma_S = \frac{1}{1 + K[R]} \tag{1b}$$

Here, the activity coefficient of the substrate, γ_s, is defined with respect to a reference state in which [R] = 0. On the other hand, K in eq 1b represents the equilibrium constant for the process

S(free) + R ⇌ S/R

(substrate linked to the receptor)　(2)

Measuring some properties at different receptor concentrations, for example, changes of the rate constants of a given reaction in which S participates, it is possible to obtain K and, from this, the standard free energy corresponding to the union substrate/receptor. Following this approach, we have done a systematic study of the interaction between a cationic metal complex, [Ru(NH$_3$)$_5$pz]$^{2+}$, and AuNPs capped with tiopronin ligands. The equilibrium binding constant K and, therefore, the free energy of binding of the ruthenium complex (positively charged) to the AuNPs were obtained following the changes in the kinetics of the electron-transfer reaction between the [Ru-(NH$_3$)$_5$pz]$^{2+}$ and S$_2$O$_8^{2-}$. From these kinetic data, a two-state model allows us to evaluate not only the strength of the binding but also its character as function of the AuNPs concentration and the ionic strength of the medium. On the other hand, working at different ionic strengths it is possible to separate
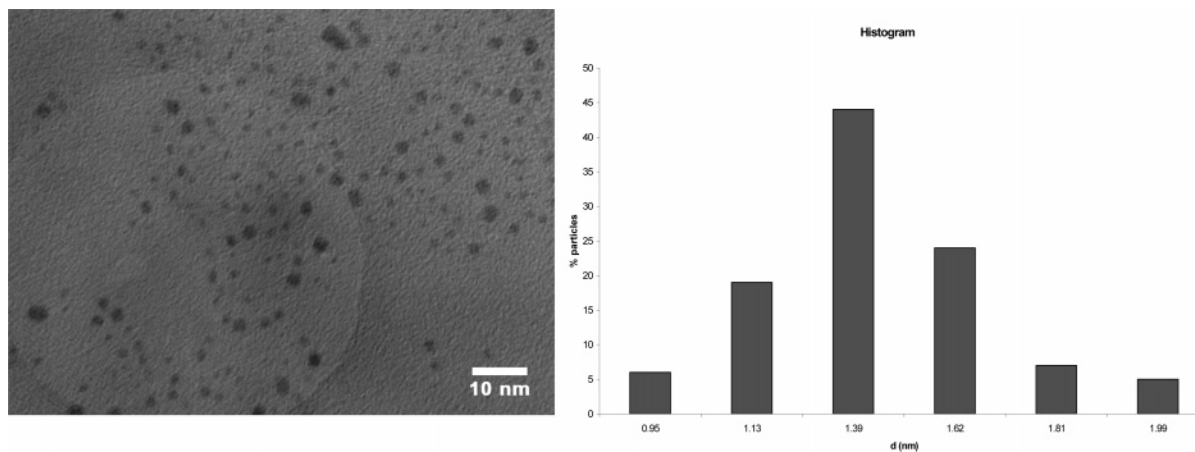
* Author to whom correspondence should be addressed. Tel.: 34-954 557177. Fax: 34-954557174. E-mail: gcjrv@us.es.
† Department of Physical Chemistry.
‡ Laboratory of Glyconanotechnology IIQ.
§ Departamento de Química Orgánica y Farmacéutica.
⊥ CIC−BiomacGUNE.

9770 *J. Phys. Chem. A, Vol. 111, No. 39, 2007*

Grueso et al.

Figure 1. Transmission electron micrograph and core size histogram of gold@tiopronin nanoparticles.

the electrostatic and nonelectrostatic contributions to the binding free energy. In this way, a complete picture of the binding can be obtained.

Materials and Methods

Materials. All chemicals were of Anal.R. grade and were used without further purification. Hydrogen tetrachloroaureate-(III) trihydrate was purchased from Sigma-Aldrich; *N*-(2-mercaptopropionyl)glycine and sodium peroxodisulphate were from Fluka; $NaBH_4$ was from Lancaster; NaCl was from Merck. $[Ru(NH_3)_5pz](ClO_4)_2$ was prepared and purified according to published procedures.[10] Solutions were prepared with deionized water, its conductivity being less than 10^{-6} S m^{-1}. Buffers were prepared according to standard laboratory procedure in order to obtain pH = 8.

Synthesis of Gold Nanoparticles: Au@tiopronin. Au@tiopronin was prepared using the procedure of Templeton et al.[11] Six batches with hydrogen tetrachloroaureate(III) trihydrate (1 equiv) and *N*-(2-mercaptopropionyl)glycine (tiopronin) (5.5 equiv) were codissolved in 12.7 mL of 6:1 methanol/acetic acid, resulting in a ruby red solution. Sodium borohydrate (22 equiv) in 2.4 mL of H_2O was subsequently added via rapid stirring. The resultant brown suspension was stirred for an additional 30 min after cooling, with the solvent removed under vacuum at 40 °C. The crude sample was completely insoluble in methanol but reasonably soluble in water. It was purified by dialysis, in which the pH of the crude product dissolved in 20 mL of water (NANOpure) was adjusted to 1 by dropwise addition of concentrated hydrochloric acid. This solution was loaded into 15 cm segments of seamless cellulose ester dialysis membrane (Sigma, MWCO = 10.000), placed in 4 L beakers of water, and stirred slowly, recharging with fresh water ca. every 10 h over the course of 72 h. The dark brown Au@tiopronin solutions were collected from the dialysis tubes and were lyophilized. The product materials were found to be spectroscopically clean and produced a yield of 119 mg.

Au@tiopronin nanoparticles were characterized by visible absorption spectra and C, H, N, S microanalysis (13.22% C; 2.09% H; 3.16% N; 7.13% S). According to this data and from the results of the transmission electron microscopy (TEM) the molecular formula was $Au_{116}(C_5H_8O_2NS)_{89}(H_2O)_{55}$. For TEM examinations, a single drop (10 μL) of the aqueous solution (0.1 mg mL^{-1}) of the AuNPs was placed onto a copper grid coated with a carbon film. The grid was left to dry in air for several hours at room temperature. TEM analysis was carried out in a Philips CM 200 electron microscope working at 200 kV.

Size distributions of the Au cores were measured from enlarged TEM image photographs for at least 80−150 individual cluster core images. Figure 1 shows a TEM image of the AuNPs. A value of 1.4 nm for the diameter of the gold nanoparticle was obtained. The UV−vis absorption spectra showed an almost nondetectable surface plasmon band (SPB) as a consequence of the small size of the clusters (Figure 2).

Spectra. The spectra of the AuNPs in the presence and in the absence of NaCl were recorded with a Cary 500 spectrophotometer at 298.2 K. No aggregation between nanoparticles was observed in the presence of the electrolyte.

Kinetic Measurements. Kinetic runs were carried out in a stopped-flow spectrophotometer from Applied Photophysics. The reaction was monitored by following the changes in absorbance of $[Ru(NH_3)_5pz]^{2+}$ at 472 nm.

All the kinetic runs were carried out under pseudo-first-order conditions using an excess of the oxidant: $[Ru(NH_3)_5pz]^{2+} = 2 \times 10^{-5}$ mol dm^{-3} and $[S_2O_8^{2-}] = 2.5 \times 10^{-4}$ mol in the reaction mixture. Pseudo-first-order rate constants were obtained from the slopes of the linear plots of $\ln(A_t - A_\infty)$ vs time, where A_t and A_∞ were the absorbances at times t and when the reaction was finished, respectively. All the experiments were repeated at least five times. The estimated uncertainty in the rate constant was less than 5%. The temperature was maintained at 298.2 ± 0.1 K.

Results

The results of the kinetic runs are shown in Tables 1−4 as pseudo-first-order rate constants. These rate constants correspond to the first electron transfer from the ruthenium complex to the peroxodisulfate:[12]

$$[Ru(NH_3)_5pz]^{2+} + S_2O_8^{2-} \rightarrow [Ru(NH_3)_5pz]^{3+} + S_2O_8^{3-}$$
$$(SO_4^{2-} + SO_4^{-\bullet}) \quad (3)$$
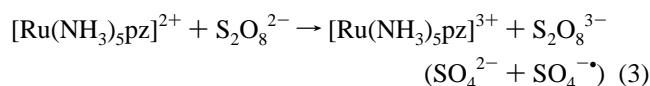
This step is slower than the second electron transfer:

$$[Ru(NH_3)_5pz]^{2+} + SO_4^{-\bullet} \rightarrow [Ru(NH_3)_5pz]^{3+} + SO_4^{2-} \quad (4)$$
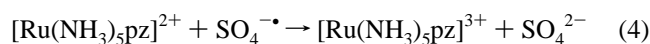
because the redox potential of the $S_2O_8^{2-/3-}$ couple is lower than that of the $SO_4^{-\bullet}/SO_4^{2-}$ couple[13] and the reorganization energy of $S_2O_8^{2-}$ is greater than that of $SO_4^{-\bullet}$.

Discussion

According to the data in Tables 1−4 the efficiency of the AuNPs for decreasing the rate of the electron-transfer reaction

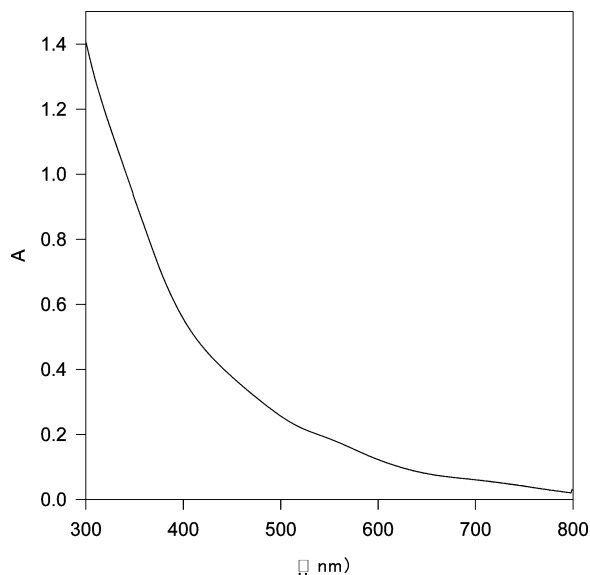Interaction between [Ru(NH₃)₅pz]²⁺ and AuNPs

J. Phys. Chem. A, Vol. 111, No. 39, 2007 **9771**

Figure 2. UV−vis spectra of Au@tiopronin nanoparticles.

TABLE 1: Rate Constants for the Reaction of $Ru(NH_3)_5pz^{2+}$ + $S_2O_8^{2-}$ at NaCl = 0 mol dm⁻³

[AuNPs]/mol dm⁻³	k/s⁻¹
0.0000	5.5
3.66×10^{-7}	4.6
7.32×10^{-7}	3.8
1.09×10^{-6}	3.1
1.83×10^{-6}	2.6
2.56×10^{-6}	1.8
3.66×10^{-6}	1.0
5.49×10^{-6}	0.62
7.32×10^{-6}	0.37

TABLE 2: Rate Constants for the Reaction of $Ru(NH_3)_5pz^{2+}$ + $S_2O_8^{2-}$ at NaCl = 0.005 mol dm⁻³

[AuNPs]/mol dm⁻³	k/s⁻¹
0.0000	4.8
3.66×10^{-7}	4.4
7.32×10^{-7}	4.1
1.09×10^{-6}	3.8
1.83×10^{-6}	3.2
2.56×10^{-6}	2.5
3.66×10^{-6}	2.0
5.49×10^{-6}	1.5
7.32×10^{-6}	1.1

TABLE 3: Rate Constants for the Reaction of $Ru(NH_3)_5pz^{2+}$ + $S_2O_8^{2-}$ at NaCl = 0.01 mol dm⁻³

[AuNPs]/mol dm⁻³	k/s⁻¹
0.0000	4.3
3.66×10^{-7}	4.1
7.32×10^{-7}	3.9
1.09×10^{-6}	3.5
1.83×10^{-6}	2.9
2.56×10^{-6}	2.6
3.66×10^{-6}	2.2
5.49×10^{-6}	1.7
7.32×10^{-6}	1.3

is clear. The *N*-(2-mercaptopropionyl)glycine is negatively charged at pH = 8. Taking into account the charges of the reactants ([Ru(NH₃)₅pz]²⁺ and S₂O₈²⁻), S would correspond to the ruthenium complex and R to the gold@tiopronin nanoparticle in eq 2.

S is distributed between the two states that appear in eq 2, free and bound. When applied to kinetics, two-state models consider a rapid distribution (in relation to the kinetic events)
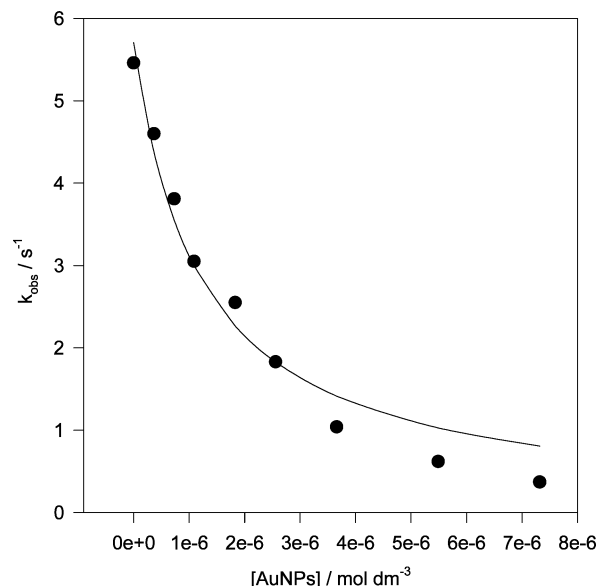

Figure 3. Plot of the experimental rate constants of the reaction Ru-(NH₃)₅pz²⁺ + S₂O₈²⁻ vs [AuNPs] concentration at [NaCl] = 0 mol dm⁻³. Symbols (●) are experimental data, and lines are the best fit using eq 7.

TABLE 4: Rate Constants for the Reaction of $Ru(NH_3)_5pz^{2+}$ + $S_2O_8^{2-}$ at NaCl = 0.02 mol dm⁻³

[AuNPs]/mol dm⁻³	k/s⁻¹
0.0000	3.4
1.09×10^{-6}	3.2
1.45×10^{-6}	3.0
1.83×10^{-6}	2.8
2.56×10^{-6}	2.7
3.66×10^{-6}	2.4
4.39×10^{-6}	2.3
5.49×10^{-6}	2.1
7.32×10^{-6}	1.8

of the reactants between two states, free and bound, to some supporting monodisperse materials, the AuNPs in this study. If the reactant is designed as Ru, an equilibrium constant K can be defined as

$$K = \frac{[Ru_B]}{[Ru_F][AuNPs]} \tag{5}$$

where Ru$_F$ represents the free state of the ruthenium complex, AuNPs is the dispersed material (or pseudophase) to which the solute binds, and Ru$_B$ represents the bound state of the solute (or the solute at the pseudophase).

Generally speaking, as the properties of the local media, or phases, corresponding to the bound and free states are different, these states react at different rates:

$$Ru_F \xrightarrow{k_F} products \tag{6a}$$

$$Ru_B \xrightarrow{k_B} products \tag{6b}$$

From eqs 5 and 6 it follows that the observed rate constant is given by[11]

$$k_{obs} = \frac{k_F + k_B K[AuNPs]}{1 + K[AuNPs]} \tag{7}$$

This equation (it is indeed the equation of the pseudophase model) opens the possibility of obtaining free energies of binding
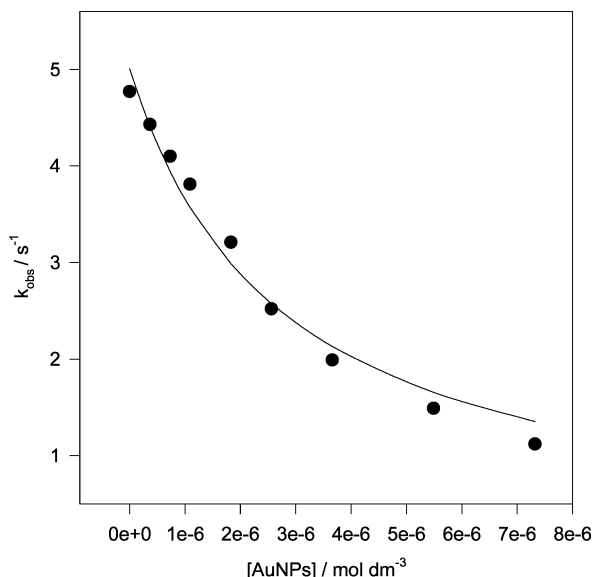
Figure 4. Plot of the experimental rate constants of the reaction Ru-$(NH_3)_5pz^{2+}$ + $S_2O_8^{2-}$ vs [AuNPs] concentration at [NaCl] = 0.005 mol dm^{-3}. Symbols (●) are experimental data, and lines are the best fit using eq 7.

**TABLE 5: Values of the Best Fit Parameters for Eq 8^a**

	K_{max}	h	j	k_F	k_B
[NaCl] = 0 M	5×10^6	9.2×10^{-6}	4.2×10^{-6}	5.7	10^{-3}
[NaCl] = 0.005 M	4.5×10^5	1.6×10^{-6}	1.2×10^{-6}	5.0	2×10^{-3}
[NaCl] = 0.010 M	$2.9 \times 10^{5\ b}$		0	4.3	0.01
[NaCl] = 0.020 M	$1.2 \times 10^{5\ b}$		0	3.4	0.1

^{a} k_F, s^{-1}; k_B, s^{-1}; j, mol dm^{-3}; h, mol dm^{-3}; K_{max}, mol^{-1} dm^3. ^{b} In this case K is independent of [AuNPs].

using specific reactions as probes.[14] This equation, in fact the Olson–Simonson equation,[15] corresponds to the behavior expected for a two-state reactive system. It is worth pointing out that, strictly speaking, eq 7 can be applied only in the case of unimolecular processes. However, as some of us have shown in a previous paper,[16] eq 7 is still valid for a second-order process provided that only one of the reactants (the [Ru(NH$_3$)$_5$-pz]$^{2+}$ complex in the present case, given the negative charge of the nanoparticles) is partitioned between the two states and the other (peroxodisulfate) remains essentially in the aqueous pseudophase.

In fact only the data in Tables 3 and 4 (corresponding to [NaCl] = 0.01 and 0.02 mol dm^{-3}, respectively) can be fitted to eq 7 with the set of parameters appearing in Table 5 (see Figures 5 and 6 where the points are experimental data and the line is the best fit obtained by using eq 7). The values of these parameters merit some comments. First of all, the values of k_w are almost the same as the values of k_{obs} in the absence of AuNPs, a fact (see Tables 3 and 4) which confirms the quality of the fit. It is also important to realize that the reactivity of the bound state is much lower than the reactivity of the free state. That is, the reaction between the ruthenium complex adsorbed on the nanoparticle and the peroxodisulfate ion is practically nonexistent. This confirms our assumption that the peroxodisulfate is practically absent at the AuNPs surface.

As to the results in the absence and in the presence of [NaCl] = 0.005 mol dm^{-3}, Figures 3 and 4 show that only the data corresponding to small ranges of the AuNPs concentrations can be fitted to eq 7. In Figures 3 and 4, the curves correspond to a fit of the experimental data by *considering K to be a true constant*, that is, independent of the AuNPs concentration. Only the first part of the curve goes through the experimental points.
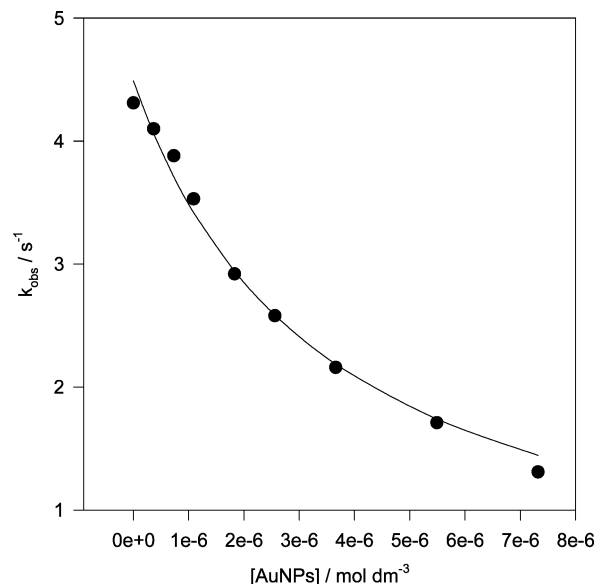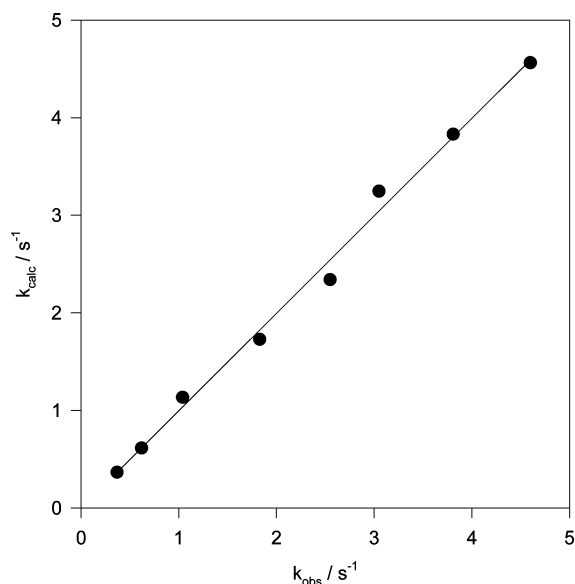

Figure 5. Plot of the experimental rate constants of the reaction Ru-$(NH_3)_5pz^{2+}$ + $S_2O_8^{2-}$ vs [AuNPs] concentration at [NaCl] = 0.01 mol dm^{-3}. Symbols (●) are experimental data, and lines are the best fit using eq 7.
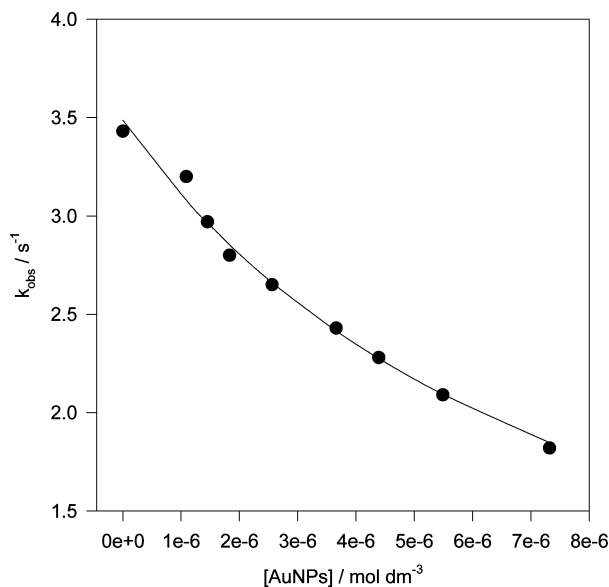
Figure 6. Plot of the experimental rate constants of the reaction Ru-$(NH_3)_5pz^{2+}$ + $S_2O_8^{2-}$ vs [AuNPs] concentration at [NaCl] = 0.02 mol dm^{-3}. Symbols (●) are experimental data, and lines are the best fit using eq 7.

As can be seen, experimental rate constants are smaller than the calculated values for the higher AuNPs concentrations. This deviation is more pronounced in the absence of NaCl and decreases at [NaCl] = 0.005 mol dm^{-3}, but it is still present as can be seen in Figure 4. That is, K changes as the AuNPs concentration changes when NaCl is not present or at the smaller NaCl concentration used.

So results corresponding to Figures 3 and 4 *cannot* be fitted by eq 7 in all the range of [AuNPs] concentrations unless allowance was made for a variation of K with the ratio between the concentrations of the [Ru(NH$_3$)$_5$pz]$^{2+}$ cation and the AuNPs. However, since the concentration of the ruthenium complex is constant in our experiments, K only depends on the concentration of the AuNPs. At first, this dependence is unknown. However to have a physical meaning K must show a saturation behavior, that is, must reach a constant value after a given

Interaction between [Ru(NH₃)₅pz]²⁺ and AuNPs

J. Phys. Chem. A, Vol. 111, No. 39, 2007 **9773**

Figure 7. Plot of the experimental rate constants of the reaction Ru-$(NH_3)_5pz^{2+}$ + $S_2O_8^{2-}$ vs calculated rate constants at [NaCl] = 0.005 mol dm^{-3} using eq 7 and K given by eq 8.

Figure 8. Plot of log K vs log[Na$^+$] (see eq 11) for the process Ru-$(NH_3)_5pz^{2+}$ + $S_2O_8^{2-}$ in AuNPs systems. The sodium from the peroxodisulphate complex (S$_2$O$_8$Na$_2$) has also been taken into account.

concentration of the nanoparticles. A dependence of K accomplishing this requirement, frequently found in many systems,[17] is given by eq 8 which corresponds to a sigmoidal dependence:

$$K = \frac{K_{max} \, e^t}{1 + e^t} \qquad (8)$$

This sigmoidal dependence is also described by the famous Hill equation[18] or the von Hippel model[19] for binding of small ligands to macromolecules. In eq 8, $t = ([AuNPs] - h)/j$, K_{max} is the maximum (limiting) value of K, h is the value of the concentration of the nanoparticles, [AuNPs], for which $K = (1/2)K_{max}$, and j is an adjustable parameter. With the use of this equation, the data in Tables 1 and 2 can be fitted in all the range of [AuNPs] concentrations used. The results of the fit are displayed in Figure 7 for [NaCl] = 0.005 mol dm^{-3}. This figure clearly indicates that our variations in K are in agreement with eq 8. Similar results are obtained in the absence of NaCl. The values of K_{max}, h, j, k_F, and k_B at [NaCl] = 0 and 0.005 mol dm^{-3} are given in Table 5.

The fact that the values of K increase when the [Ru(NH₃)₅-pz]$^{2+}$/[AuNPs] decreases means that the union of the ruthenium complex and the nanoparticles is anticooperative. This fact implies that, in comparison with higher ionic strength, the AuNPs not only change the strength of binding but also its character: it is noncooperative in the case of [NaCl] = 0.01 and 0.02 mol dm^{-3} and anticooperative in the absence of NaCl and at [NaCl] = 0.005 mol dm^{-3}.[19] This anticooperative character has also been observed in the case of the binding of small ions to DNA,[20] peptides,[21] and dendrimers.[22] Of course, part of this anticooperativity arises as a consequence of the fact that, when one complex is bound, a second complex would feel repulsion from the first bound one. In the presence of added electrolyte (NaCl here) an ionic cloud will be developed around the particles (and the adsorbed ruthenium complexes). This ionic cloud would produce a screening of another Ru(NH₃)₅pz^{2+} ion coming toward the particle, and more so when the concentration of added salt increases, in such a way that the anticooperative character of the binding, caused by the repulsive interactions of the ligands, would decrease. However, other causes of
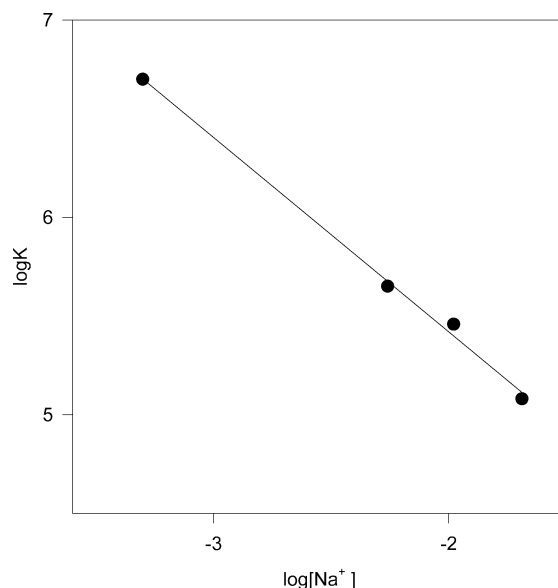
anticooperativity cannot be ruled out. Thus, the binding of a ruthenium complex, with a charge sign opposite from the charge of the nanoparticle, would produce a screening between the charges on the tiopronin ligands in the AuNPs, allowing in this way a more compact conformation of the receptor, with different binding properties from those related to the less compact conformation in the absence of the ruthenium complex.

The values of the equilibrium binding constant obtained for each NaCl concentration also allow an estimation of the nonelectrostatic and electrostatic components of the binding. This will be shown as follows: K (or K_{max}) can be expressed in function of the free energy corresponding to the process in eq 2. Without any loss of generality, this free energy, ΔG, can be written as the sum of two contributions: (i) an electrostatic potential independent contribution, ΔG_{nel} (nonelectrostatic or intrinsic), and (ii) an electrostatic potential dependent contribution, ΔG_{el} (electrostatic). This separation has been discussed extensively in references 23–27:

$$\Delta G = \Delta G_{nel} + \Delta G_{el} \qquad (9)$$

Thus, the free energy of binding ΔG can be written as a sum of two contributions: a nonelectrostatic contribution, ΔG_{nel}, and an electrostatic one, ΔG_{el}, which implies

$$K = K_{nel}K_{el} \qquad (10)$$

In order to separate these contributions we used the Lippard's equation. According to Howe-Grant and Lippard,[27] log K_{el} is proportional to $-$log[Na$^+$], that is,

$$\log K = \log K_{nel} - \beta \log[Na^+] \qquad (11)$$

The values of log K (or K_{max}) appearing in Table 5 are plotted in Figure 8. In order to calculate [Na$^+$], the sodium from the peroxodisulfate (Na$_2$S$_2$O$_8$) has also been taken into account. From the intercept, a value of log $K_{nel} = 3.4$ is found which gives a value of 2.5×10^3 mol^{-1} dm^3 for K_{nel}. That is, taking into account the values of K (or K_{max}) appearing in Table 5 ($K_{max} = K$ when the binding is noncooperative), it can be established that the nonelectrostatic component of the free energy of binding is about a half of the total free energy in the
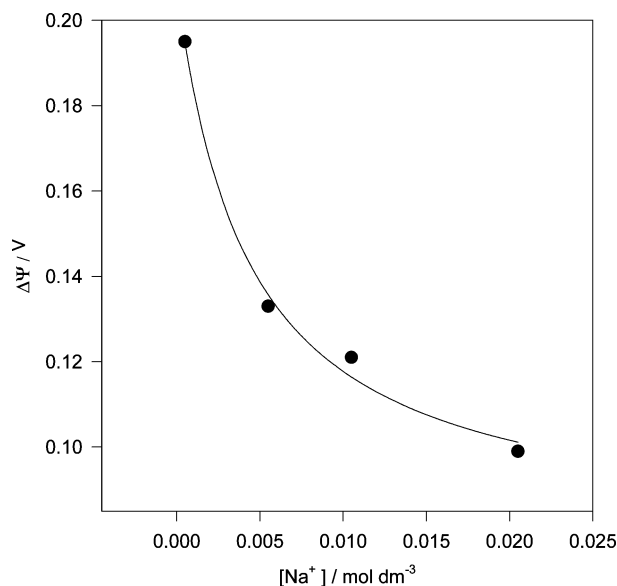
Figure 9. Plot of $\Delta\Psi$/V vs $[Na^+]$/mol dm^{-3}.

absence of NaCl and about 67% of the total free energy of binding in the presence of NaCl 0.02 mol dm^{-3}. From the slope of the plot in Figure 8 a value of 0.98 for β was obtained. This value, close to unity, would imply that the adsorption sites are the same for Na^+ and $[Ru(NH_3)_5pz]^{2+}$, independent of their charge. Notice that this substitution would imply a net increase of the charge of the particle/ligand that would make more difficult the approximation of a second $[Ru(NH_3)_5pz]^{2+}$, thus giving rise to the observed anticooperativity.

Once the value of K_{nel} (2.5×10^3 mol^{-1} dm^3) has been determined, K_{el} for each $[Na^+]$ concentration can be obtained as $K_{el} = K/K_{nel}$ (see eq 10). From K_{el}, taking into account that

$$\ln K_{el} = \frac{-nF\Delta\Psi}{RT} \tag{12}$$

where $\Delta\Psi$ is the electrostatic potential difference at the AuNPs interface, this parameter can be easily obtained. The values of $\Delta\Psi$ at different $[Na^+]$ are given in Figure 9. It is interesting to note that the values of $\Delta\Psi$ are of the same order of size as those existing at the interfaces of micelles.[28]

In conclusion, the binding of the complex $[Ru(NH_3)_5pz]^{2+}$ to gold@tiopronin nanoparticles has been studied following a kinetic approach. It has been shown that the character and strength of the binding of the cations to AuNPs is dependent on the ionic strength of the aqueous phase in contact with the gold@tiopronin nanoparticle. When the ionic strength increases (i) there is a partial neutralization of the charge on the AuNPs, in such a way that the free energy of binding increases, and thus K_{max} decreases and (ii) the effect of the ruthenium complex on AuNPs, which causes the anticooperative character of the binding, becomes less important, a fact which permits the

modulation of this noncovalent interaction. This is so because the same effect is produced by the cations of the supporting electrolyte which are present at a (constant) concentration much higher than that of the ruthenium complex. This effect seems to be "saturated" at ionic strengths of about 0.01 mol dm^{-3}. On the other hand, working at different NaCl concentrations the nonelectrostatic and electrostatic contributions to the binding free energy have been separated. From the latter, we have obtained the values of the electrostatic potential differences at the AuNPs/solutions interface.

References and Notes

(1) Barrientos, A. G.; de la Fuente, J. M.; Rojas, T. C.; Fernandez, A.; Penades, S. *Chem.—Eur. J.* **2003**, *9*, 1909.
(2) Aslan, K.; Pérez-Luna, V. H. *Plasmonics* **2006**, *1*, 111.
(3) Bi-Feng, P.; Feng, G.; Li-Mei, A. *J. Magn. Magn. Mater.* **2005**, *293* (1), 252.
(4) Akbulut, M.; Alig, A. R. G.; Younjin, M.; Belman, N.; Reynolds, M.; Golan, Y.; Israelachvili, J. *Langmuir* **2007**, *23* (7), 3961.
(5) Khomutov, G. B.; Koksharov, Y. A. *Adv. Colloid Interface Sci.* **2006**, *122* (1−3), 119.
(6) Niemeyer, C. M. *Angew. Chem., Int. Ed.* **2001**, *40*, 4128.
(7) Cliffel, D. E.; Zamborini, F. P.; Gross, S. M.; Murray, R. W. *Langmuir* **2000**, *16*, 9699.
(8) De la Fuente, J. M.; Berry, C. C.; Riehle, M. O.; Curtis A. S. G. *Langmuir* **2006**, *22*, 3286.
(9) (a) Muriel-Delgado, F.; Jiménez, R.; Gómez-Herrera, C.; Sánchez, F. *Langmuir* **1999**, *15*, 4334. (b) Davies, K.; Hussam, A. *Langmuir* **1993**, *9*, 3270.
(10) Creutz, C.; Taube, H. *J. Am. Chem. Soc.* **1973**, *95*, 1086.
(11) Templeton, A. C.; Chen, S.; Gross, S. M.; Murray, R. W. *Langmuir* **1999**, *15*, 66.
(12) Fürholz, U.; Haim, A. *Inorg. Chem.* **1987**, *26*, 3243.
(13) Eberson, L. In *Electron Transfer Reactions in Organic Chemistry*; Springer-Verlag: New York, 1987; p 88.
(14) Villa, I.; Prado-Gotor, R. *Chem. Phys. Lett.* **2007**, *434*, 210.
(15) Olson, A. R.; Simonson, J. R. *J. Phys. Chem.* **1949**, *17*, 1167.
(16) Lopez-Cornejo, P.; Sánchez, F. *J. Phys. Chem. B* **2001**, *105*, 10523.
(17) Hammes, G. G. In *Thermodynamics and Kinetics for the Biological Sciences*; Wiley-Interscience: New York, 2000; p 124 ff.
(18) Haynie, D. T. *Biological Thermodynamics*; Cambridge University Press: Cambridge, UK, 2001; p 233.
(19) Mc Ghee, J. D.; Von Hippel, P. H. *J. Mol. Biol.* **1974**, *86*, 469.
(20) Secco, F.; Venturini, M.; López, M.; Pérez, P.; Prado, R.; Sánchez, F. *Phys. Chem. Chem. Phys.* **2001**, *3*, 4412.
(21) Chavanieu, A.; Guichou, J. F.; Prado-Gotor, R.; Pérez-Tejeda, P.; Jiménez, R.; López-Cornejo, P.; Sánchez, F. *J. Phys. Chem. B* **2005**, *109*, 19676.
(22) de la Vega, R.; Pérez-Tejeda, P.; Prado-Gotor, R.; López-Cornejo, P.; Jiménez, R.; Pérez, F.; Sánchez, F. *Chem. Phys. Lett.* **2004**, *398*, 82.
(23) Dolcet, C.; Rodenas, E. *Can. J. Chem.* **1990**, *68*, 932.
(24) Ortega, F.; Rodenas, E. *J. Phys. Chem.* **1987**, *91* 837.
(25) Bunton, C. A.; Moffat, J. R. *J. Phys. Chem.* **1986**, *90*, 538.
(26) Al-Lohedan, H. A. *J. Chem. Soc., Perkin Trans 2* **1995**, 1707.
(27) Howe-Grant, M.; Lippard, S. J. *Biochemistry* **1979**, *18*, 5762.
(28) Bernas, A.; Grand, D.; Hautecloque, S.; Giannotti, C. *J. Phys. Chem.* **1986**, *90*, 6189.